

## COMPACT BANDPASS FILTER USING FOLDED LOOP RESONATOR WITH HARMONIC SUPPRESSION

**B. Jitha, P. C. Bybi, C. K. Aanandan, P. Mohanan and K. Vasudevan**

Cochin University of Science and Technology  
India

**Abstract**—A novel compact microstrip bandpass filter using folded open loop resonator is presented. The resonator elements are placed in close proximity to parallel coupled microstrip lines. The presence of undesired harmonics is eliminated here by properly modifying the configuration of the folded resonator. The measured and simulated results are in good agreement.

### 1. INTRODUCTION

In microwave communication systems, compact bandpass filters having low insertion loss in the passband together with high attenuation in the stopband are desirable. The conventional parallel coupled microstrip bandpass filter though widely used, suffers from spurious responses generated at the multiples of resonant frequency for which different methods have been proposed [1–8] to eliminate them. In [1, 2] the odd mode phase length is extended by overlapping the coupled lines on to the resonator. The phase velocity equalization is obtained by methods such as suspended substrate [3], floating strip conductors in the ground plane [4] and over coupling technique with size miniaturization by capacitive termination [5]. The technique proposed in [6] to cancel the difference between even and odd mode velocities is by adding a centered floating conductor in the slotted ground plane below the coupled line sections. But very few papers have addressed the issue of multi-spurious response suppression. Recently suppression of multiple spurious responses was achieved by tuning the coupled-line sections to the different bands to be rejected [7]. The suppression of second and third harmonics is achieved with quarter wavelength resonators in the bandpass filter using basic loop resonators in [8] where the

---

Corresponding author: C. K. Aanandan (aanandan@gmail.com).

miniaturization was accomplished by folding the loop resonators and selectivity improved by generating transmission zeros by vias.

In this paper a compact loop resonator bandpass filter with a good rejection in the stopband is proposed. The technique adopted here to reduce the size is to fold the resonator without affecting its resonant frequency. Apart from reducing size, the folding results in the generation of anti resonant modes which could be excited by introducing a slit in the loop. To suppress the higher order harmonics, the length of coupling between the resonator and the transmission line is adjusted to produce transmission zeroes at  $2f_0$  and  $3f_0$ . The performance of the filter is evaluated using simulation and experiment.

## 2. BANDPASS FILTER DESIGN

Figure 1 shows folded loop resonator obtained by folding the closed loop resonator so that the perimeter of the loop remains the same.

Loop resonators have the bandpass characteristics when placed between the input and output feed lines. Resonance occurs when standing waves are set up in the resonator; this happens when its perimeter is an integral multiple of the guided wavelength. In the case of conventional closed loop resonator,

$$n\lambda_g = p_{av} \quad (1)$$

where  $\lambda_g$  is the guided wavelength,  $n$  is the mode number and  $p_{av}$  is the average perimeter of the closed loop (shown by dotted lines in the Figure).

For a microstrip loop,  $\lambda_g$  can be related to the frequency by

$$\lambda_g = \frac{\lambda}{\sqrt{\epsilon_{eff}}} = \frac{1}{\sqrt{\epsilon_{eff}}} \frac{c}{f} \quad (2)$$

where  $c$  is the speed of light and  $\epsilon_{eff}$  is the effective dielectric constant.

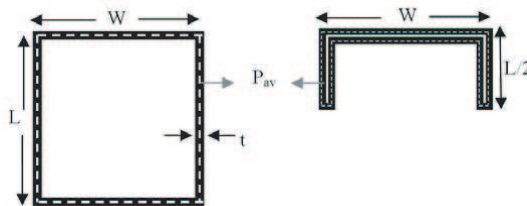


**Figure 1.** Folded closed loop from conventional closed loop resonator.

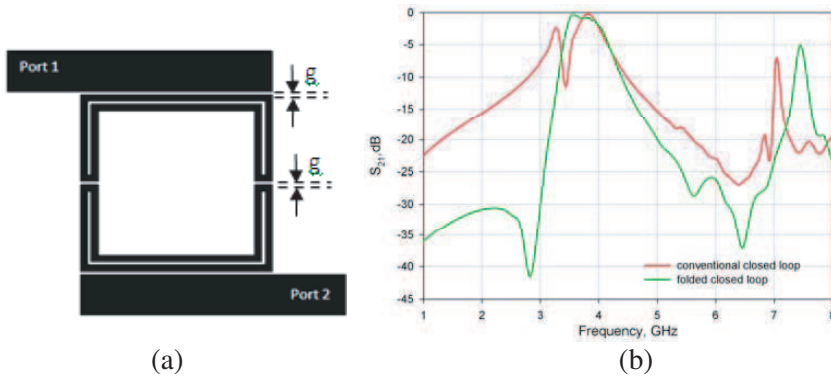


**Figure 2.** (a) Folded closed loop resonator filter. (b) Frequency response comparing the conventional closed loop and folded loop resonator filter.

Equation (1) becomes

$$f = \frac{nc}{p_{av}\sqrt{\epsilon_{eff}}} \quad \text{for } n = 1, 2, 3, \dots \quad (3)$$

and

$$\epsilon_{eff} = \frac{\epsilon_r + 1}{2} \quad (4)$$

The new filter structure shown in Fig. 2(a) has two folded closed loop resonators etched on FR4 substrate and arranged in such a way that the perimeter of the resultant structure is same as that of a single square closed loop. The metal width  $t$  ( $= 0.5 \text{ mm}$ ) and the gap distance  $d = g$  ( $= 0.2 \text{ mm}$ ), are kept small to get a narrow passband. The filter is simulated using Ansoft HFSS and the  $S$ -parameters comparing the frequency responses of conventional closed loop resonator and the folded loop resonator are shown in Fig. 2(b).

As can be seen from the plot, modified structure resonates at the same frequency as that of the conventional square loop resonator with a second resonance at twice the resonant frequency. Consequently the same design equation of the closed loop resonator may be used. In order to understand the basic phenomenon underlying the operation of this folded loop, the field configurations for different modes are examined. The magnitude of  $E$  field distribution at the two resonant modes is shown in Fig. 3.

The plot in Fig. 3(a) shows a full wave variation within each folded closed loop and that in Fig. 3(b) consists of two full waves confined in each of the loops indicating the higher mode ( $n = 2$ ). The Fig. 4 shows the corresponding phase plots of the above filter.

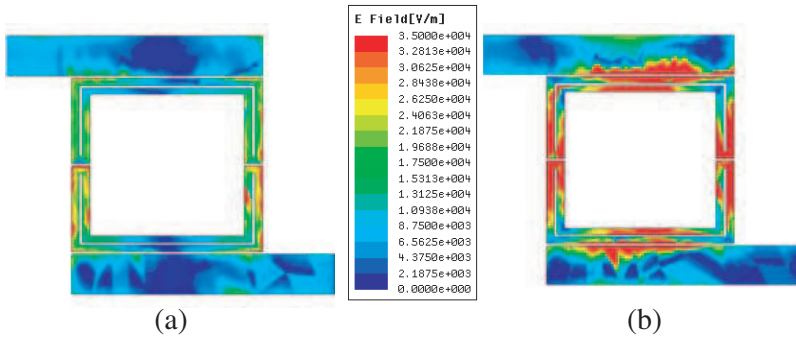


**Figure 3.**  $E$  field distribution at (a) 3.8 GHz, (b) 7.5 GHz.

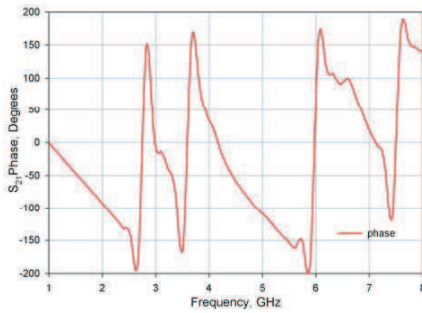


**Figure 4.** Phase plot of the folded closed loop resonator filter.

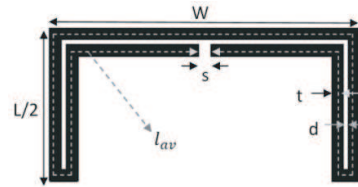
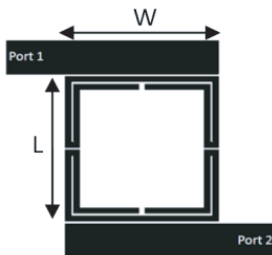
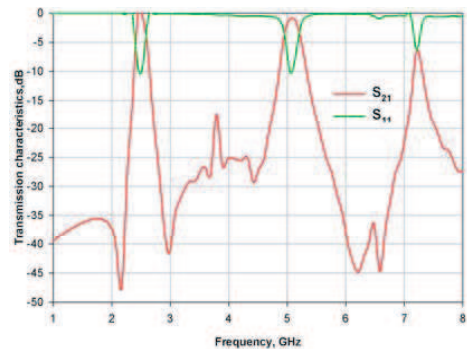


**Figure 5.** Layout of the folded open loop resonator.



(a)



(b)

**Figure 6.** (a) Bandpass filter employing folded open loop resonators ( $L \times W = 13 \times 13 \text{ mm}^2$ ). (b) Simulated transmission characteristics.

It can be observed from the plot, there are abrupt phase changes at four frequencies indicating possibility of four resonances. However, there are only two resonances observed in Fig. 3. The frequencies which are absent in the plot in Fig. 3 (i.e., around 2.6 GHz and 6 GHz) are the anti resonant frequencies that are blocked by the folded loop resonator. These frequencies can be excited by forced boundary conditions such as opening or shorting the loop. The open boundary condition is obtained by introducing a slit in the loop and the resultant folded open loop resonator shown in Fig. 5.

The frequency response of the parallel coupled folded open loop resonator filter (Fig. 6(a)) is shown in Fig. 6(b) which depicts a passband at 2.53 GHz which was blocked by the folded closed loop resonator.

From the above predictions and observations, the resonant frequency of the folded open loop resonator can be given as

$$f_0 \approx \frac{n + 1}{c} \left( \frac{c}{l_{av} \sqrt{\epsilon_{eff}}} \right) \quad \text{for } n = 1, 3, 5, \dots \quad (5)$$

where  $l_{av}$  is the average length of the open loop.

From these equations, the resonant frequencies for different modes can be calculated. It is evident from the plot that the resonance at 3.8 GHz and 6.5 GHz are suppressed which are the modes corresponding to mode number  $n = 2$  and  $n = 4$ .

The relation in (3) is validated by designing the filter on different dielectric substrates for resonant frequencies 1, 2 and 4 GHz and compared with the simulated frequency in Table 1.

The effect of slit width on the resonant frequency has been studied by simulating the structure with varying  $s$ . The plot in Fig. 7 depicts a small shift in passband frequency with the slit width and thus can be considered for fine tuning of the filter response. The variation in upper transmission zero is due to the variation in overall capacitance of the resonator with slit width.

**Table 1.** Comparison of calculated and simulated frequencies.

$f_{cal}$ (GHz)	$\epsilon_r = 2.2$		$\epsilon_r = 4.4$		$\epsilon_r = 10.2$	
	$l_{av}$ (mm)	$f_{sim}$ (GHz)	$l_{av}$ (mm)	$f_{sim}$ (GHz)	$l_{av}$ (mm)	$f_{sim}$ (GHz)
1	159	1.04	122	1.0	85	1.0
2	79	2.06	61	2.0	42.6	2.06
4	40	4.08	30.5	4.0	21.3	4.0

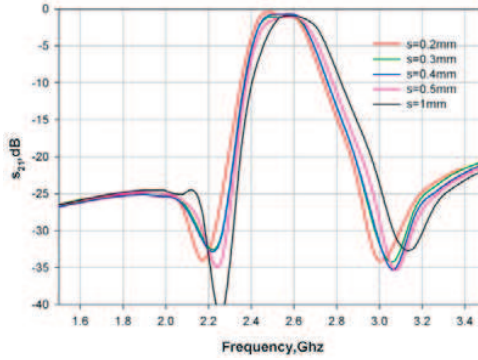


**Figure 7.** Simulation results for filter with varying slit width.

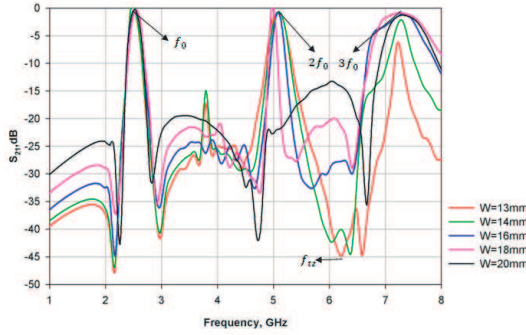


**Figure 8.** Simulated  $S_{21}$  characteristics for different values of  $W$ .

While the configuration is compact and has sharper roll-off than the parallel coupled conventional closed resonator filters, it suffers from the spurious responses which can be suppressed by altering the length of coupling between the microstrip and the folded resonator.

Increasing the coupling length ( $W$ ) of the folded resonator with the coupling microstrip line, the passband will be almost unchanged, moving the transmission zero  $f_{tz}$  to lower frequency. The second harmonics is eliminated when the transmission zero frequency ( $f_{tz}$ ) becomes lower than  $2f_0$ . That is,

$$W \approx l_{t1} > \frac{\lambda_g}{4} \quad (6)$$

The characteristics of the proposed filter with different coupling lengths are shown in Fig. 8. It is worth noticing that as the coupling length is increased to  $W = 20 \text{ mm} > \frac{\lambda_g}{4}$  which is half wave length at  $2f_0$ , the transmission zero shifts to the lower frequency removing the second harmonics.

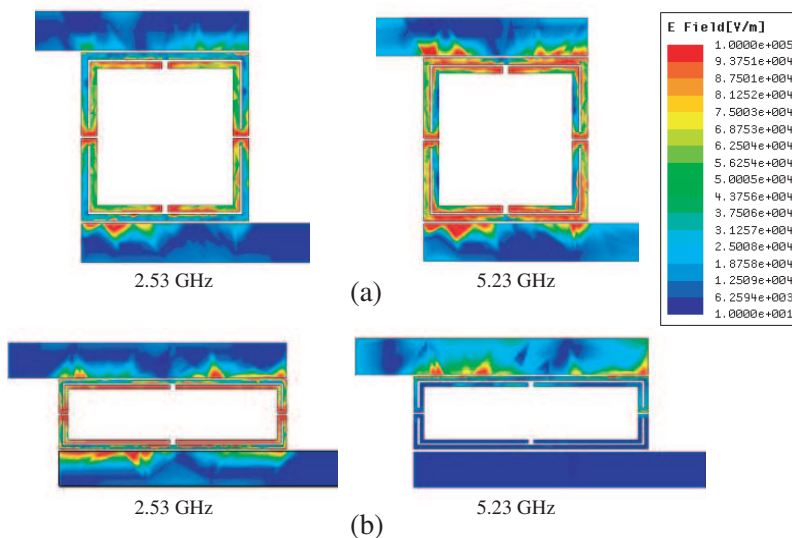


**Figure 9.**  $E$ -field distribution at 2.53 GHz and 5.23 GHz for (a)  $W = 13$  mm, (b)  $W = 20$ mm.

To compare the field distribution of the two configurations with and without second harmonics, the  $E$  field distribution plot have been obtained for the  $W = 13$  mm and  $W = 20$  mm at 2.53 GHz and 5.23 GHz. They are shown in Fig. 9.

The plot in Fig. 9(a) shows propagation in both the first and second harmonics, whereas the lower figure depicts clearly the absence of field concentration in the loop resonator and the output feed line at 5.23 GHz. That is, the loop resonator is electromagnetically invisible at the second resonance since it exhibit no field density, and thus coupling zero fields to the output port.

The next higher harmonics rejection is accomplished when the coupling length of the microstrip line in the lower part  $l_{t2}$  of the resonator is shorter than  $\frac{\lambda_g}{4}$  or when approximately equal to half guide wavelength at  $3f_0$ . The coupling length of the output microstrip line  $l_{t2}$  is

$$l_{t2} \simeq \frac{2}{3} \left( \frac{\lambda_g}{4} \right) \tag{7}$$

Figure 10(a) shows the schematic of the bandpass filter based on the above design whose simulated characteristics are shown in Fig. 10(b).

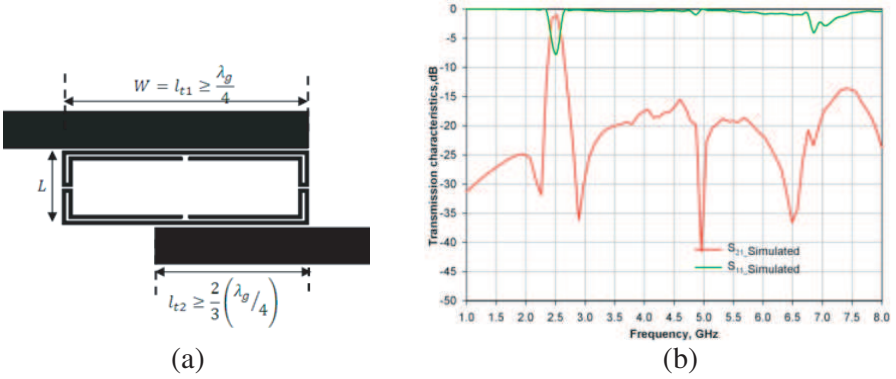


**Figure 10.** (a) Layout of the proposed filter ( $W \times L = 20 \times 6$ ,  $g = d = 0.2$  mm,  $s = 0.5$  mm,  $t = 0.5$  mm). (b) Simulated transmission characteristics.

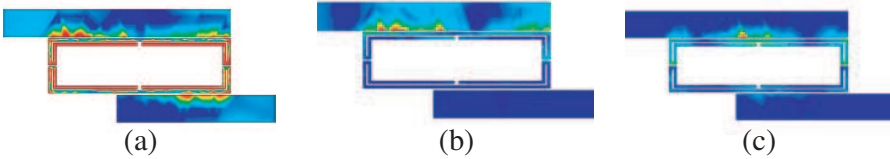


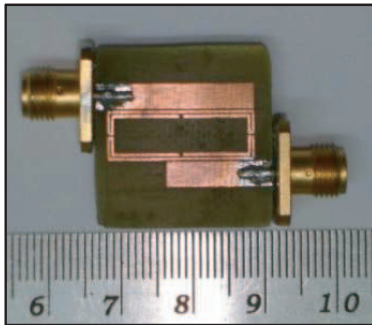
**Figure 11.**  $E$  field distribution at frequencies (a) 2.53 GHz, (b) 5.23 GHz, (c) 7.48 GHz.

The field distribution plots at 2.53, 5.23 and 7.48 GHz have been simulated to verify the effect of coupling length of the input and output feed lines which produces transmission zeros at their corresponding resonant frequencies. The field distribution in loop resonators of Figs. 11(b) and (c) are not illuminated confirming the absence of field distribution and propagation.

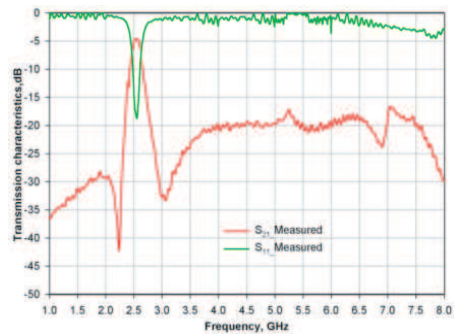
In order to verify the theoretical predictions, the filter is designed and optimized to operate at 2.5 GHz, fabricated on FR4 substrate ( $\epsilon_r = 4.4$ ,  $h = 1.6$  mm) is shown in Fig. 12. The occupied area (without considering the feed lines) is only  $0.17\lambda_0 \times 0.05\lambda_0$  ( $\lambda_0$  is the free space wavelength at operating frequency). The performance of the filter is experimentally verified using HP8510c Network analyzer. A passband ( $-10$  dB) of about 230 MHz with good out of band suppression is obtained.

Good agreement is seen between both simulated (Fig. 10(b)) and measured results (Fig. 12(b)), with a clear rejection of propagation in the vicinity of two harmonic frequencies. Around the center

frequency of 2.53 GHz, the measured insertion loss and the return loss are approximately 4.56 dB and 20 dB respectively; the high value of insertion loss can be attributed mainly to the dielectric losses and fabrication error as the simulation results show only 0.95 dB on a loss less substrate. The suppression of the spurious harmonics is around 20 dB.



(a)



(b)

**Figure 12.** (a) Photograph of the proposed filter. (b) Measured transmission characteristics.

### 3. CONCLUSION

A novel compact microstrip bandpass filter based on folded loop resonator is presented with a good rejection in the stopband. The higher harmonics are suppressed by modifying the configuration of the resonator. The compact design and sharp out of band rejection make it suitable for modern communication systems.

### ACKNOWLEDGMENT

The authors acknowledge the UGC, Govt of India, for financial assistance.

### REFERENCES

1. Riddle, A., "High performance parallel coupled microstrip filters," *IEEE MTT-s Int. Microwave Symp. Dig.*, 427–430, 1988.
2. Kuo, J., S. Chen, and M. Jiang, "Parallel coupled microstrip filters with over coupled end stages for suppression of responses," *IEEE*

- Microwave and Wireless Component Letters*, Vol. 13, No. 10, 440–442, 2003.
3. Kuo, J.-T., M. Jiang, and H. J. Chang, “Design of parallel coupled microstrip filters with suppression of spurious resonances using substrate suspension,” *IEEE Trans. Microwave Theory Tech.*, Vol. 52, No. 1, 83–89, 2004.
  4. Velazquez, M. C., J. Marel, and F. Medina, “Parallel coupled microstrip filters with floating grounding plane conductor for spurious — Band suppression,” *IEEE Trans. Microwave Theory Tech.*, Vol. 53, No. 5, 1823–1828, 2005.
  5. Cheong, P., S.-W. Fok, and K.-W. Tam, “Miniaturised parallel coupled — Line bandpass filter with spurious-response suppression,” *IEEE Trans. Microwave Theory Tech.*, Vol. 53, No. 5, 1810–1816, 2005.
  6. Velazquez-Ahumada, M. C., J. Martel-Villagr, and F. Medina, “Microstrip coupled line filters with spurious band suppression,” *PIERS Online*, Vol. 3, No. 6, 948–950, 2007.
  7. Lopetegi, T., M. A. G. Laso, F. Falcone, F. Martin, J. Bonache, J. Garcia, L. Perez-Cuevas, M. Sorolla, and M. Guglielmi, “Microstrip wiggly-line bandpass filters with multispurious rejection,” *IEEE Microwave and Wireless Component Letters*, Vol. 14, No. 11, 531–533, 2004.
  8. Lin, H.-N., W.-L. Huang, and J.-L. Chen, “Miniaturization of harmonics-suppressed filter with folded loop structure,” *PIERS Online*, Vol. 4, No. 2, 238–244, 2008.